Sensor and Simulation Notes

Note 208

January 1975

# Analysis of Modes in a Finite-Width Parallel-Plate Waveguide

T. Itoh and R. Mittra
Electromagnetics Laboratory
Department of Electrical Engineering
University of Illinois at Urbana-Champaign
Urbana, Illinois 61801



## Abstract

An efficient method has been developed for analyzing modal characteristics of a finite-width parallel-plate waveguide. The method is based on an extension of Galerkin's procedure applied in the Fourier transform domain. Numerical values of propagation constants and field distributions have been obtained for various structural and modal parameters.

This study was performed under subcontract to

The Dikewood Corporation
1009 Bradbury Drive, S.E.
University Research Park
Albuquerque, New Mexico 87106

CONTENTS

ILLUSTRATIONS

TABLES

# SECTION I

# INTRODUCTION

Parallel-plate transmission lines are often employed as a guiding structure for electromagnetic pulse (EMP) simulators. This type of transmission line, as shown in figure 1, has in addition to the dominant TEM mode an infinite number of higher-order modes. Because of the open nature of the structure, the propagation constants of these higher-order modes are usually complex, representing the propagation as well as radiation loss of the modes. When an object to be tested is placed in the present structure, it is illuminated by electromagnetic waves consisting of a combination of TEM and a number of higher-order modes. The scattered field is also a superposition of TEM and higher-order modes. Hence, the nature of the higher-order modes in the parallel-plate transmission line is worth investigating and the development of a computer program to obtain the propagation constant and the modal field distribution is important for EMP studies.

The problem of parallel-plate transmission lines has been studied by several workers (refs. 1 and 2) using various approaches. In this paper, a new method is presented for attacking this problem. The method is an extension of Galerkin's procedure in the spectral domain. The original version of this method, which has been applied to many microstrip-type transmission line structures (refs. 3 and 4), is extended here to apply to the structure with complex transverse propagation constants. In the following sections, the formulation of the problem, numerical procedures, and some results are presented.

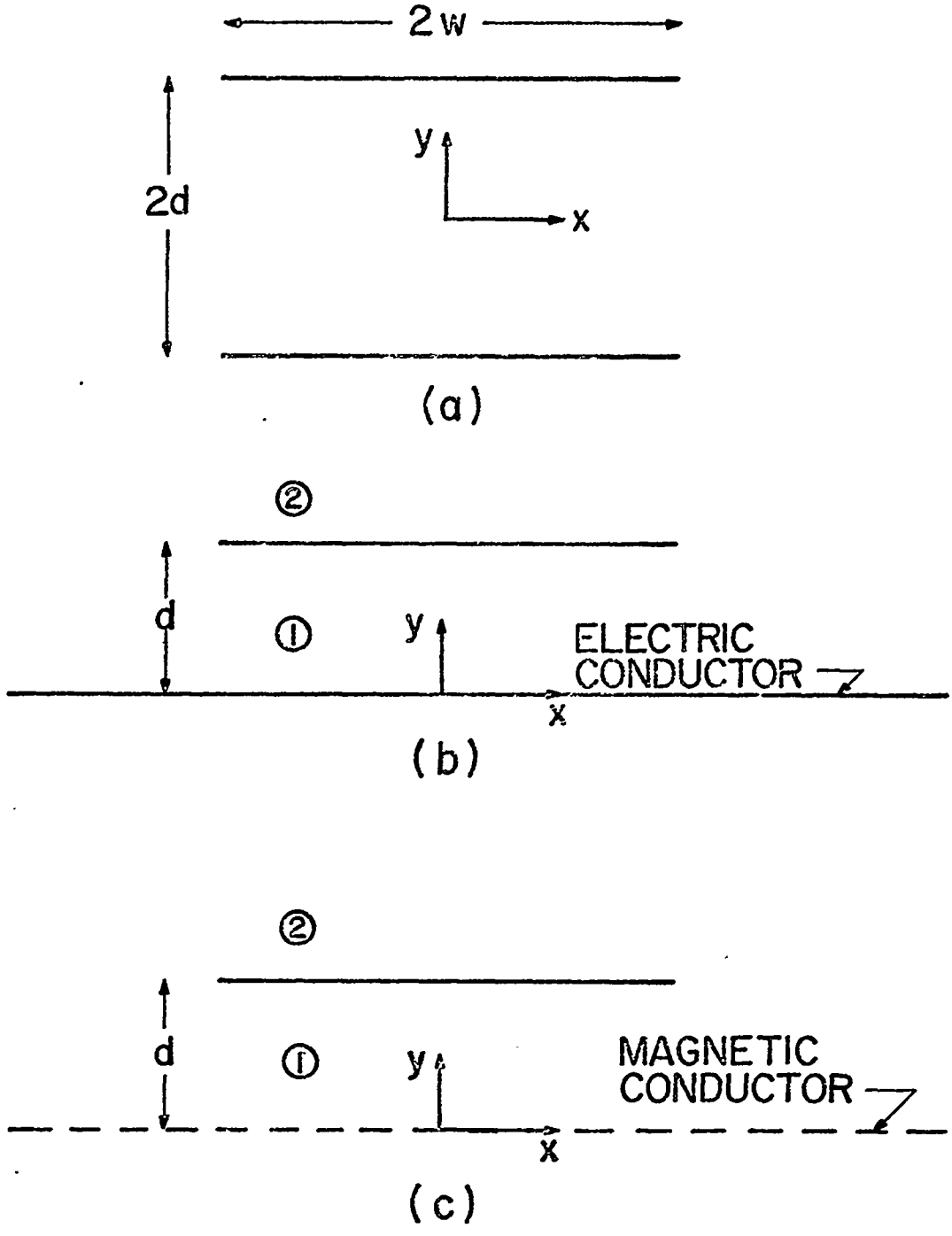


Figure 1. (a) Cross Section of a Finite-Width Parallel-Plate Waveguide (b), (c) Equivalent Structure.

## SECTION II

## FORMULATION OF THE PROBLEM

The cross section of the parallel-plate transmission line is shown in figure 1. Assume that the plates are infinitely thin and that both the plates and the medium are lossless. It is well known that the dominant mode in this structure is TEM with the propagation constant identical to the free-space wave number. All of the higher-order modes may be classified into the two sets, TM and TE, with respect to the z-direction. Assuming $\exp(j\omega t - j\beta z)$ variation, where the propagation constant $\beta$ is complex, in general, all of the field components of the TM and TE modes may generally be expressed in terms of scalar potentials as

TM modes

$$\left.\begin{aligned} E_z &= j\,\frac{k^2 - \beta^2}{\beta}\,\phi(x,y) \\ E_x &= \frac{\partial\phi}{\partial x} \qquad E_y = \frac{\partial\phi}{\partial y} \\ H_x &= -\frac{\omega\varepsilon_0}{\beta}\,\frac{\partial\phi}{\partial y} \qquad H_y = \frac{\omega\varepsilon_0}{\beta}\,\frac{\partial\phi}{\partial x} \end{aligned}\right\} \tag{1}$$

TE modes

$$\left.\begin{aligned} H_z &= j\,\frac{k^2 - \beta^2}{\beta}\,\psi(x,y) \\ E_x &= \frac{\omega\mu_0}{\beta}\,\frac{\partial\psi}{\partial y} \qquad E_y = -\frac{\omega\mu_0}{\beta}\,\frac{\partial\psi}{\partial x} \\ H_x &= \frac{\partial\psi}{\partial x} \qquad H_y = \frac{\partial\psi}{\partial y} \end{aligned}\right\} \tag{2}$$

where $k = 2\pi/\lambda$ is the free-space wave number, and $\varepsilon_0$ and $\mu_0$ are the permittivity and permeability of free space, respectively. The common factor $\exp(j\omega t - j\beta z)$ has been and will be omitted throughout this paper.

In addition to the TE and TM classification, the symmetry of the structure allows us to further subclassify the modal spectrum. For instance, the symmetricity of the direction of the z-component of induced current on the plates allows us to subclassify the spectrum into the four cases listed in table 1. The detailed formulation will now be given for Cases 1 and 3 of TM modes only (odd TM modes), and only the resultant equations will be summarized for the rest of the cases. Because of the nature of the present method of analysis, the distinction between Cases 1 and 3 (and between Cases 2 and 4) is not necessary in the formulation process.

Table 1

CLASSIFICATION BY SYMMETRICITY

| Case | $x > 0, y > 0$ | $x < 0, y > 0$ | $x < 0, y < 0$ | $x > 0, y < 0$ |
|---|---|---|---|---|
| 1 | + | + | - | - |
| 2 | + | + | + | + |
| 3 | + | - | - | + |
| 4 | + | - | + | - |

\+ $J_z$ flows in the positive z direction

\- $J_z$ flows in the negative z direction

Such distinction is undertaken only at the stage of preparation for numerical computation.

In the odd TM mode cases, it is only necessary to consider the equivalent structure shown in figure 1(b) where the $y = 0$ plane is an electric conductor. Since the structure is infinite in the x-direction, the electromagnetic boundary value problem is formulated in the spectral or Fourier transform domain as opposed to the conventional space domain formulation (refs. 3 and 4).

To this end, let us define the Fourier transform $\tilde{\phi}(\alpha,y)$ of the scalar potential $\phi(x,y)$ via

$$\tilde{\phi}_i(\alpha,y) = \int_{-\infty}^{\infty} \phi_i(x,y)\ e^{j\alpha x}\, dx \tag{3}$$

where i = 1 and 2 designates the regions $0 < y < d$ and $y > d$, respectively. The transforms of field components may be defined from equations (1) and (3) as

$$\left.\begin{aligned} \tilde{E}_{zi} &= j\,\frac{k^2 - \beta^2}{\beta}\,\tilde{\phi}_i(\alpha,y) \\ \tilde{E}_{xi} &= -j\alpha\,\tilde{\phi}_i(\alpha,y) \\ \tilde{H}_{xi} &= -\frac{\omega\varepsilon_0}{\beta}\,\frac{\partial}{\partial y}\,\tilde{\phi}_i(\alpha,y) \end{aligned}\right\} \tag{4}$$

Since $\phi_i$ satisfies the wave equation, $\tilde{\phi}_i$ is a solution of

$$\left(\frac{d^2}{dy^2} - \gamma^2\right)\tilde{\phi}_i(\alpha,y) = 0 \tag{5}$$

where

$$\gamma^2 = \alpha^2 + \beta^2 - k^2 \tag{6}$$

Because of the boundary conditions $E_z = E_x = 0$ at $y = 0$ and the radiation condition at $y \to +\infty$, the solution of equation (5) is

$$\tilde{\phi}_1(\alpha,y) = A(\alpha)\ \sinh \gamma y \qquad 0 < y < d \tag{7a}$$

$$\tilde{\phi}_2(\alpha,y) = B(\alpha)\ \exp[-\gamma(y - d)] \qquad y > d \tag{7b}$$

where A and B are unknowns. Note that Re $\gamma > 0$ and Im $\gamma > 0$ are to be satisfied so that equation (7b) represents a valid form for $y \to +\infty$.

The next step is to apply the interface conditions at y = d in the transform domain. Since

$$E_{z1}(x,d-) = E_{z2}(x,d+) \qquad \text{all } x$$

$$E_{x1}(x,d-) = E_{z2}(x,d+) \qquad \text{all } x$$

$$H_{x1}(x,d-) = H_{x2}(x,d-) \qquad |x| > w$$

the interface conditions expressed in the transform domain are

$$\tilde{E}_{z1}(\alpha,d-) = \tilde{E}_{z2}(\alpha,d+) \tag{8}$$

$$\tilde{E}_{x1}(\alpha,d-) = \tilde{E}_{x2}(\alpha,d+) \tag{9}$$

$$\tilde{H}_{x1}(\alpha,d-) - \tilde{H}_{x2}(\alpha,d+) = \tilde{J}_z(\alpha) \tag{10}$$

where $\tilde{J}_z$ is the transform of the z-directed, unknown, induced current on the plate at y = d. Substitution of equations (4) and (7) into equation (8) gives the relation between A and B. Equation (9) is automatically satisfied for A and B. If these quantities are substituted in equation (10), A or B is expressed in terms of another unknown $\tilde{J}_z(\alpha)$.

$$B(\alpha) = \tilde{G}_0(\alpha)\ \tilde{J}_z(\alpha) \tag{11}$$

where

$$\tilde{G}_0(\alpha,\beta) = \frac{-\beta}{\omega\varepsilon_0\gamma[1 + \coth \gamma d]} \tag{12}$$

Now, the final boundary condition $E_z(x,d) = 0$ for $|x| < w$ is imposed in the transform domain. Since $E_z(x,d)$ is unknown but nonzero for $|x| > w$, it can be written as

$$E_z(x,d) = \begin{cases} 0 \\ \\ j\,\dfrac{k^2 - \beta^2}{\beta}\,u(x) \end{cases} \tag{13}$$

Hence, the transform is

$$\tilde{E}_z(\alpha,d) = j\,\frac{k^2 - \beta^2}{\beta}\,\tilde{U}(\alpha) \tag{14}$$

where

$$\tilde{U}(\alpha) = \int_{-\infty}^{-w} u(x)\; e^{j\alpha x}\,dx + \int_{w}^{\infty} u(x)\; e^{j\alpha x}\,dx$$

Eliminating $B(\alpha)$ from equations (8), (11) and (14), obtain

$$\tilde{G}_0(\alpha,\beta)\;\tilde{J}_z(\alpha) = \tilde{U}(\alpha) \tag{15}$$

It should be mentioned that equation (15) is the transform of the integral equation of the convolution form encountered in many conventional space domain analyses. It may also be worthwhile to mention that equation (15) contains two unknowns, $\tilde{J}_z$ and $\tilde{U}$; however, it is possible that in the solution one of the unknowns, $\tilde{U}$, may be eliminated and that equation (15) is solved for $\tilde{J}_z$ only.

Before concluding this section, let us summarize the resultant equations for other symmetries and polarizations.

TM, even in y (Cases 2 and 4 in table 1)

$$\tilde{G}_e(\alpha,\beta)\;\tilde{J}_z(\alpha) = \tilde{U}(\alpha) \tag{16a}$$

$$\tilde{G}_e = \frac{-\beta}{\omega\varepsilon_0\gamma[1 + \tanh\,\gamma d]} \tag{16b}$$

TE, odd in y

$$\tilde{L}_0(\alpha,\beta)\ \tilde{J}_z(\alpha) = \tilde{V}(\alpha) \tag{17a}$$

$$\tilde{L}_0(\alpha) = \frac{\gamma\beta}{j(k^2 - \beta^2)[1 + \coth \gamma d]} \tag{17b}$$

TE, even in y

$$\tilde{L}_e(\alpha,\beta)\ \tilde{J}_z(\alpha) = \tilde{V}(\alpha) \tag{18a}$$

$$\tilde{L}_e(\alpha) = \frac{\gamma\beta}{j(k^2 - \beta^2)[1 + \tanh \gamma d]} \tag{18b}$$

For TE cases,

$$\tilde{V}(\alpha) = \int_{-\infty}^{-w} v(x)\ e^{j\alpha x}\, dx + \int_{w}^{\infty} v(x)\ e^{j\alpha x}\, dx \tag{19a}$$

$$v(x) = \frac{\partial}{\partial y} H_z(x,d) \quad . \tag{19b}$$

## SECTION III

## METHOD OF SOLUTION

In this section, a method of solving algebraic equation (15) is discussed. The method, which is applicable to solving equations (16a), (17a), and (18a) as well, is based on Galerkin's procedure applied in the Fourier transform domain.

The first step expands the unknown $\tilde{J}_z(\alpha)$ in terms of known basis functions $\tilde{J}_n(\alpha)$, $n = 1, \ldots, N$.

$$\tilde{J}_z(\alpha) = \sum_{n=1}^{N} c_n \tilde{J}_n(\alpha) \tag{20}$$

where $c_n$'s are unknown coefficients to be determined. The choice of $\tilde{J}_n(\alpha)$'s is such that they are the Fourier transforms of appropriate functions with finite support, viz., $J_n(x)$'s, the inverse transforms of $\tilde{J}_n(\alpha)$'s, are zero for $|x| > w$.

Substituting equation (20) into equation (15) and taking an inner product of the resultant equation with one of $\tilde{J}_m(\alpha)$'s, $m = 1,2, \ldots, N$, one obtains

$$\sum_{n=1}^{N} K_{mn}(\beta)\, c_n = 0 , \quad m = 1,2, \ldots, N \tag{21}$$

where

$$K_{mn}(\beta) = \int_{-\infty}^{\infty} \tilde{J}_m(\alpha)\, \tilde{G}_0(\alpha,\beta)\, \tilde{J}_n(\alpha)\, d\alpha \tag{22}$$

The right-hand side of equation (21) is zero using Parseval's relation

$$\int_{-\infty}^{\infty} \tilde{J}_m(\alpha)\, \tilde{U}(\alpha)\, d\alpha = \frac{\beta}{j(k^2 - \beta^2)} \int_{-\infty}^{\infty} J_m(-x)\, E_z(x,d)\, dx \equiv 0$$

because $J_m$ and $E_z$ are nonzero only over complementary regions of x.

When $J_n(x)$'s, whose transforms are to be used as basis functions $\tilde{J}_n(\alpha)$'s, are chosen, they must satisfy certain symmetry requirements in addition to being zero for $|x| > w$. For instance, in Case 1 in table 1, $J_n(x)$'s must be symmetric with respect to the y axis, while in Case 3 they are required to be antisymmetric. Furthermore, it is desirable to use $J_n(x)$'s which well represent the edge condition at $x = \pm w$ where the actual z-directed current shows square integrable singularity. Using these basis functions, equation (21) is solved for unknown propagation constant $\beta$ which is usually a complex number.

After $\beta$ is obtained, the field distribution may be calculated as follows. Except for the normalization factor, the ratio of all $c_n$'s is determined, which gives the current distribution

$$J_z(x) = \sum_{n=1}^{N} c_n J_n(x) \tag{23}$$

The field distribution of $E_z$ may be obtained from equations (7), (11), (15) and (20).

$$E_z(x,y) = \begin{cases} j \dfrac{k^2 - \beta^2}{\beta} \displaystyle\sum_{n=1}^{N} c_n \int_{-\infty}^{\infty} \frac{\sinh \gamma y}{\sinh \gamma d} \tilde{G}_0(\alpha)\, \tilde{J}_n(\alpha)\, e^{-j\alpha x}\, d\alpha & 0 < y < d \quad (24a) \\ j \dfrac{k^2 - \beta^2}{\beta} \displaystyle\sum_{n=1}^{N} c_n \int_{-\infty}^{\infty} \exp[-\gamma(y - d)]\, \tilde{G}_0(\alpha)\, \tilde{J}_n(\alpha)\, e^{-j\alpha x}\, d\alpha & y > d \quad (24b) \end{cases}$$

All the higher-order TE and TM modes in the present structure may be designated by a set of numbers (p,q) for each symmetric subgroup. The number p is associated with the field variation in the x direction and number q for the variation in the y direction. In the present method, p can be predetermined by the appropriate choice of basis functions $\tilde{J}_n$ for the current distribution

on the plate. However, there is no built-in process to choose q in the analysis procedure. Rather, q is controlled in the numerical process of finding $\beta$ by the judicious choice of a starting point in the root-seeking algorithm.

## SECTION IV

## NUMERICAL PROCEDURE

A numerical algorithm has been developed for TM modes of Case 1 with the mode index p = 0. This choice of p corresponds to the higher-order modes with the least field variation in the x-direction. The basis functions have been selected so that the qualitative nature of the actual current is well represented. Specifically the following functions have been employed:

$$J_1(x) = \begin{cases} 1 & |x| < w \\ 0 & \text{otherwise} \end{cases} \tag{25}$$

$$J_2(x) = \begin{cases} 1 + \left|\frac{x}{w}\right| & |x| < w \\ 0 & \text{otherwise} \end{cases} \tag{26}$$

The basis functions for equation (21) are the Fourier transforms of equations (25) and (26), which are

$$\tilde{J}_1(\alpha) = \frac{2 \sin \alpha w}{\alpha} \tag{27}$$

$$\tilde{J}_2(\alpha) = \frac{4 \sin \alpha w}{\alpha} - \frac{2}{\alpha^2 w} (1 - \cos \alpha w) \tag{28}$$

Although any number of functions similar to these given by the above equations could be used as a set of basis functions, N in equation (21) was set to two. Only two basis functions (27) and (28) were employed for economic reasons, that is, for minimizing the computer time. It was found, however, that quite satisfactory answers were obtained for many microstrip problems by using only one or two basis functions of the type similar to equations (27) and (28) (ref. 4).

Equations (27) and (28) are substituted into equation (22) to numerically compute $K_{mn}$'s, and complex roots $\beta$ of

$$\det\left|K_{mn}(\beta)\right| = 0 \tag{29}$$

are found by a complex root-seeking algorithm. This algorithm finds the closest zero from a given starting point. At this stage, only the mode number p is given and another mode number q is left undecided. It is possible to correlate the value of q and the appropriately chosen starting point of the algorithm.

The starting values of the route-seeking routine have been chosen in the following way. The present structure can be viewed as a fictitious closed waveguide with sidewalls with complex surface impedance. For well-guided modes, these sidewalls may be very close to the magnetic walls since, for such modes, the radiation loss may be quite small. Hence, the propagation constant $\beta_s$ of waveguides with magnetic sidewalls may be chosen as a starting point of the algorithm. (See figure 2.) For the present mode spectrum of Case 1 and TM, $\beta_s$ may be given from figure 2a

$$\beta_s = \sqrt{k^2 + \alpha_s^2} \tag{30}$$

$$\alpha_s^2 = -\left(\frac{p\pi}{w}\right)^2 - \left(\frac{q\pi}{d}\right)^2, \quad p = 0, 1, 2, \ldots$$

$$q = 1, 2, \ldots$$

Note that we are concerned with p = 0 modes in the present numerical computations using equations (27) and (28) for basis functions.

It is hoped in the numerical algorithm that the zero of equation (29) closest to the value of $\beta_s$ be obtained for a given q; such a zero is called the propagation constant $\beta_{pq}$ of the $TM_{pq}$ mode of Case 1.

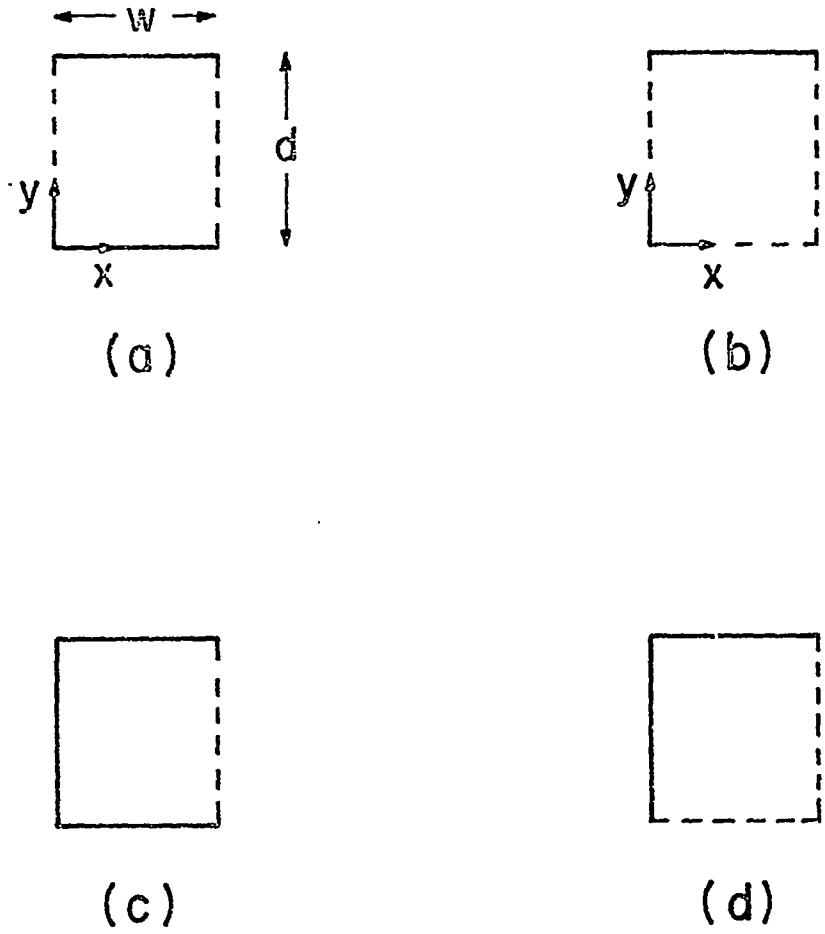


Figure 2. Classification by Symmetry for the Determination of the Starting Value of β.

## SECTION V

## NUMERICAL RESULTS

Some typical computer solutions are summarized in table 2 with d, w and the wavelength $\lambda$ being input parameters. Also, the p = 0 and q values are specified.

In many EMP problems, the so-called transverse propagation constant $\alpha_{pq}$ is more preferable than the propagation constant $\beta_{pq}$ (ref. 1). The definition of $\alpha_{pq}$ is

$$\sqrt{k^2 + \alpha_{pq}^2} = \beta_{pq} \tag{31}$$

The transverse propagation constant $\alpha_{pq}$ here corresponds to $p_n$ given in ref. 1. Notice, however, that unlike in ref. 1, $\alpha$ as well as $\beta$ carries two indices p and q because the structure in the present case has non-negligible plate width.

The magnitudes of the $E_z$ field in the waveguide cross section, which are computed using equation (24), are plotted in figure 3. It is clear that the field decays away from the waveguide in both the x- and y-directions. Although $|E_z|$ must be zero on the plate at y = d, the numerical results did not predict that it would be zero, but would approach zero. It is hoped that these values approach zero as the number of basis functions are increased. It is also seen that the number of peaks in the y direction for $0 < y < d$ coincides with the given value of q.

Table 2

COMPUTER SOLUTIONS OF PROPAGATION CHARACTERISTICS

(0,1) MODE

| $\frac{w}{d}$ | $\frac{d}{\lambda}$ | $2\beta_s d$ | $2\beta_{pq} d$ | $2\alpha_{pq} d$ | No. Iter. |
|---|---|---|---|---|---|
| 2.5 | 2 | 24.32 - j2.432 | 21.76 - j0.114 | -.1972 + j12.58 | 16 |
| 10 | 1 | 10.88 - j1.088 | 10.82 - j0.0652 | -.1104 + j6.382 | 5 |
| 5 | 2 | 24.32 - j2.432 | 21.72 - j0.0448 | -.0728 + j12.644 | 12 |
| 3.33 | 3 | 37.17 - j3.717 | 20.82 - j0.0335 | -.0222 + j31.428 | 45 |
| 2.5 | 4 | 49.84 - j4.984 | 55.92 - j6.68 | -27.28 + j13.696 | 15 |
| 2 | 5 | 62.5 - j6.25 | 54.1 - j0.163 | -.276 + j31.96 | 24 |
| 5 | 10 | 125.5 - j12.55 | 107.2 - j14.72 | -22.28 + j70.80 | 7 |
| 5 | 5 | 62.5 - j6.25 | 59.6 - j14.5 | -28.46 + j30.36 | 25 |
| 5 | 3.33 | 41.4 - j4.14 | 45.8 - j11.78 | -25.52 + j21.14 | 29 |
| 5 | 2.5 | 30.8 - j3.08 | 34.4 - j3.94 | -15.92 + j8.52 | 8 |
| 5 | 2 | 24.4 - j2.44 | 21.8 - j0.045 | -.078 + j12.50 | 12 |
| 5 | 1.67 | 19.98 - j1.998 | 16.74 - j0.060 | -.080 + j12.58 | 12 |
| 5 | 1.11 | 12.46 - j1.246 | 12.36 - j0.021 | -.040 + j6.50 | 5 |
| 5 | 1 | 10.88 - j1.088 | 10.78 - j0.044 | -.074 + j6.46 | 5 |
| 2 | 1 | 10.88 - j1.088 | 10.29 - j0.044 | -.063 + j7.22 | 8 |
| 1 | 2 | 24.32 - j2.432 | 19.28 - j0.068 | -.081 + j16.12 | 15 |
| 0.67 | 3 | 37.2 - j3.72 | 50.88 - j12.66 | -36.3 + j17.70 | 27 |

(0,2) MODE

| | | | | | |
|---|---|---|---|---|---|
| 10 | 1 | 0.2 - j0.02* | 0.078 - j0.88 x $10^{-4}$ | -7.6 x $10^{-7}$ + j9.56 | 12 |

*The actual $2\beta_s d$ was 0.0 - j0.0. However, $2\beta_s d$ was shifted to 0.2 - j0.02 for numerical convenience.

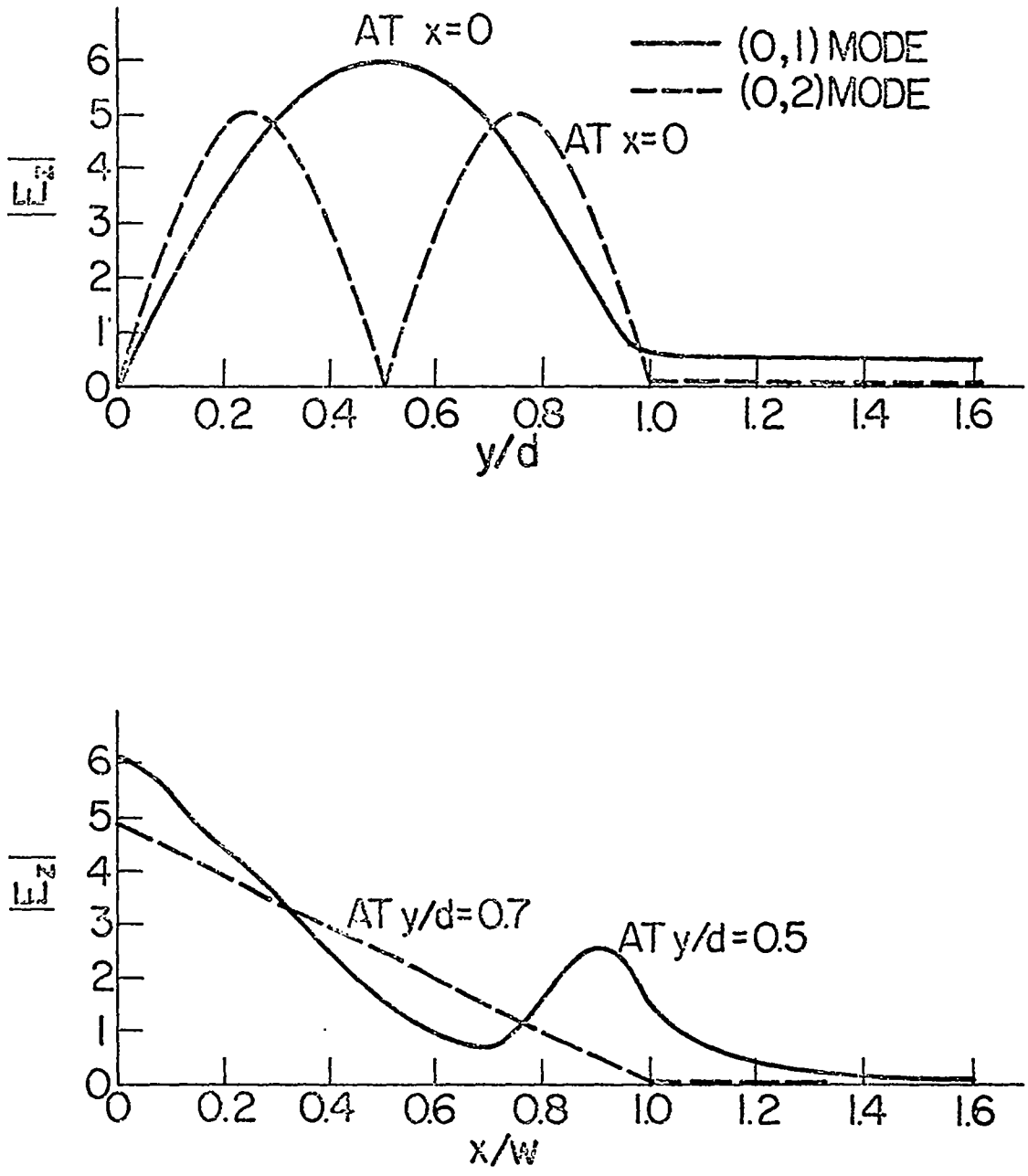


Figure 3. Field Distribution in the Cross Section of the Waveguide

## SECTION VI
## CONCLUSIONS

A simple and efficient numerical method has been developed for analyzing a finite-width parallel-plate waveguide. Sample computations based on this method predicted the propagation constants of the modes in such a structure and the field plots so obtained have shown the expected physical nature of these modes.

## REFERENCES


1. Marin, L., "Modes on a Finite-Width, Parallel-Plate Simulator. I. Narrow Plates," Sensor and Simulation Notes No. 201, Dikewood Corporation, September 1974.

2. Liu, T. K., "Impedance and Field Distributions of Curved Parallel-Plate Transmission-Line Simulators," Sensor and Simulation Notes No. 170, Dikewood Corporation, February 1973.

3. Itoh, T. and Mittra, R., "Dispersion Characteristics of the Slot Lines," Electronics Letters, 7, 13, pp. 364-365, July 1971.

4. Itoh, T. and Mittra, R., "Spectral Domain Approach for Calculating the Dispersion Characteristics of Microstrip Lines," IEEE Trans. Microwave Theory Tech., MTT-21, 7, pp. 496-499, July 1973.